Fixation Can Change the Appearance of Phase Separation in Living Cells

Shawn Irgen-Gioro[1], Victoria Walling[1], Shasha Chong[1]*

[1] *Division of Chemistry and Chemical Engineering, California Institute of Technology, Pasadena, CA 91125, USA*

* Correspondence: schong@caltech.edu

Abstract

Fixing cells with paraformaldehyde (PFA) is an essential step in numerous biological techniques as it is thought to preserve a snapshot of biomolecular transactions in living cells. Fixed cell imaging techniques such as immunofluorescence have been widely used to detect liquid-liquid phase separation (LLPS) *in vivo*. Here, we compared images, before and after fixation, of cells expressing intrinsically disordered proteins that are able to undergo LLPS. Surprisingly, we found that PFA fixation can both enhance and diminish putative LLPS behaviors. For specific proteins, fixation can even cause their droplet-like puncta to artificially appear in cells that do not have any detectable puncta in the live condition. Fixing cells in the presence of glycine, a molecule that modulates fixation rates, can reverse the fixation effect from enhancing to diminishing LLPS appearance. We further established a kinetic model of fixation in the context of dynamic protein-protein interactions. Simulations based on the model suggest that protein localization in fixed cells depends on an intricate balance of protein-protein interaction dynamics, the overall rate of fixation, and notably, the difference between fixation rates of different proteins. Our work reveals that PFA fixation changes the appearance of LLPS from living cells, presents a caveat in studying LLPS using fixation-based methods, and suggests a mechanism underlying the fixation artifact.

Introduction

Fixing cells to preserve a snapshot of biomolecular transactions *in vivo* is a widely used strategy in numerous techniques in biology and medicine. Due to its small size and high reactivity with a wide range of biological entities, paraformaldehyde (PFA) is one of the most commonly used fixatives to create covalent cross-linking between biomolecules, e.g., proteins and nucleic acids. PFA non-selectively "fixes" or cross-links molecules in proximity to enable characterization of biomolecular interactions formed in living cells. Examples of popular techniques that use PFA to fix cells include ChIP-sequencing (Solomon and Varshavsky, 1985), chromosome conformation capture (3C) based techniques (Quinodoz et al., 2018), immunofluorescence (Richter et al., 2018), fluorescence in situ hybridization (FISH) (Moter and Göbel, 2000), cross-linking mass spectrometry (Sutherland et al., 2008), super-resolution expansion microscopy (Chen et al., 2015), and super-resolution localization microscopies such as stochastic optical reconstruction microscopy (STORM) (Rust et al., 2006). Although PFA fixation has been used to faithfully preserve live-cell conditions in many scenarios, a number of studies have uncovered situations in which fixation fails to cross-link DNA-protein interactions formed in living cells. By imaging different transcription factors (TFs) in live and fixed cells, Schmiedeberg et al. showed that TFs bound to DNA with fast dissociation dynamics (<5 sec residence times as determined by fluorescence recovery after photobleaching (FRAP)) are not cross-linked to DNA upon PFA fixation (Schmiedeberg et al., 2009). Using live-cell single-molecule imaging, Teves et al. showed that TFs stay bound to chromosome during mitosis and fixing cells can artificially deplete transiently bound TFs from mitotic chromosomes (Teves et al., 2016). These studies exemplify the fact that fixation, with limited reaction rates, cannot provide an

instantaneous snapshot and may miss or obfuscate biomolecular interactions that happen either at or faster than the timescale of fixation. What further complicates the result of cell fixation is that the reactivity and reaction rates of PFA are variable and dependent on its biomolecule substrates (Gavrilov et al., 2015; Shishodia et al., 2018). For example, the efficiency and rates at which PFA reacts with proteins can vary by orders of magnitude (Kamps et al., 2019) and are dependent on their amino acid sequences (Kamps et al., 2019; Metz et al., 2004; Sutherland et al., 2008) and tertiary structures (Hoffman et al., 2015).

Among the numerous biomolecular transactions investigated using fixed cell imaging is liquid-liquid phase separation (LLPS), a long-observed behavior of polymers in solution (Gibbs, 1879; Graham, 1861; Hyman et al., 2014) that has recently generated much excitement in biological research communities due to its proposed roles in cellular organization and functions (Banani et al., 2017; Boeynaems et al., 2018; Mitrea and Kriwacki, 2016; Shin and Brangwynne, 2017). LLPS is driven by excessive levels of transient, selective, and multivalent protein-protein interactions mediated by intrinsically disordered regions (IDRs) within the proteins of interest (Chong et al., 2018; Kato and McKnight, 2018; Li et al., 2012). Whereas rigorous characterization of LLPS *in vivo* has been challenging and remains a question under active investigation (McSwiggen et al., 2019), detecting local high-concentration regions of an endogenously expressed protein using immunofluorescence of fixed cells has been used in many studies as evidence of LLPS occurring under physiological conditions (Hayes and Weeks, 2016; Kato et al., 2012; Lin et al., 2016; Maharana et al., 2018; Sabari et al., 2018; Wang et al., 2021; Yang et al., 2020). However, fixation has only been assumed, but not directly shown, to faithfully preserve multivalent interactions and LLPS formed in living cells. This knowledge gap motivated us to image cells that overexpress various IDR-containing proteins before and after fixation to evaluate the ability of PFA fixation to preserve LLPS behaviors. We found that interestingly, fixation can significantly alter the appearance of droplet-like puncta in cells. Our quantitative image analysis suggests that depending on the LLPS-driving protein, fixing cells can either enhance or diminish the apparent LLPS behaviors *in vivo*. In certain cases, fixation can even cause droplet-like puncta to artificially appear in cells that have a homogeneous protein distribution and no detectable puncta in the live condition. Conversely, fixation can also cause droplet-like puncta in living cells to completely disappear. Combining experiments that modulate fixation rates and simulations based on a kinetic model, we further demonstrated that protein localization in fixed cells depends on an intricate balance of protein-protein interaction dynamics, the overall rate of fixation, and the difference between protein fixation rates in and out of droplet-like puncta. Our work urges caution in the interpretation of previous claims of *in vivo* phase separation based solely on immunofluorescence imaging of fixed cells and serves to guide future judicious application of PFA fixation.

Results

Fixation Enhances the LLPS Appearance of FET Family Proteins

To investigate the effect of PFA fixation on the appearance of LLPS, we first compared confocal fluorescence images of live and fixed U2OS cells that transiently express an IDR tagged with EGFP and a nuclear localization sequence (NLS). We focused on the FET family protein IDRs (AA2-214 of FUS, AA47-266 of EWS, and AA2-205 of TAF15) that are reported to undergo putative LLPS in cells upon overexpression (Altmeyer et al., 2015; Chong et al., 2018; Kato et al., 2012; Kwon et al., 2013; Schuster et al., 2020; Wang et al., 2018; Zheng et al., 2020). **Figure 1, Video 1, and Figure 1–figure supplement 1**

compare the same cells before and after treatment of 4% PFA for 10 minutes, a typical condition utilized for fixed cell imaging techniques such as immunofluorescence (Stadler et al., 2010). At high enough expression levels, all three IDRs are able to form discrete and spherical puncta in the live cell nucleus, which show fusion and fission behaviors and are thereby consistent with LLPS droplets (Alberti et al., 2019; Banani et al., 2017; Choi et al., 2020; Li et al., 2012). Interestingly, after fixation, the puncta of all three IDRs appear to increase in their numbers, sizes, and contrast compared with the dilute phase. In particular, PFA fixation was able to artificially turn a cell with EGFP-EWS(IDR) homogeneously distributed in the nucleus without any puncta into one with many discrete puncta (**Figure 1A**). We quantified the fixation-induced changes of LLPS appearance by calculating three parameters from the fluorescence images of cells, including the number of puncta, surface roughness, and punctate fraction, and found a significant increase in all three parameters after fixation (**Figure 1D-F**). The number of puncta and punctate fraction (percentage of intranuclear protein molecules in the concentrated phase) are indicators of the propensity to phase separate (Berry et al., 2015). The surface roughness (standard deviation of pixel intensities across the nucleus) quantifies the uneven distribution of a fluorescently labeled protein in the nucleus, allowing for detection of puncta appearance or disappearance without the need for an algorithm to identify individual puncta in the cell.

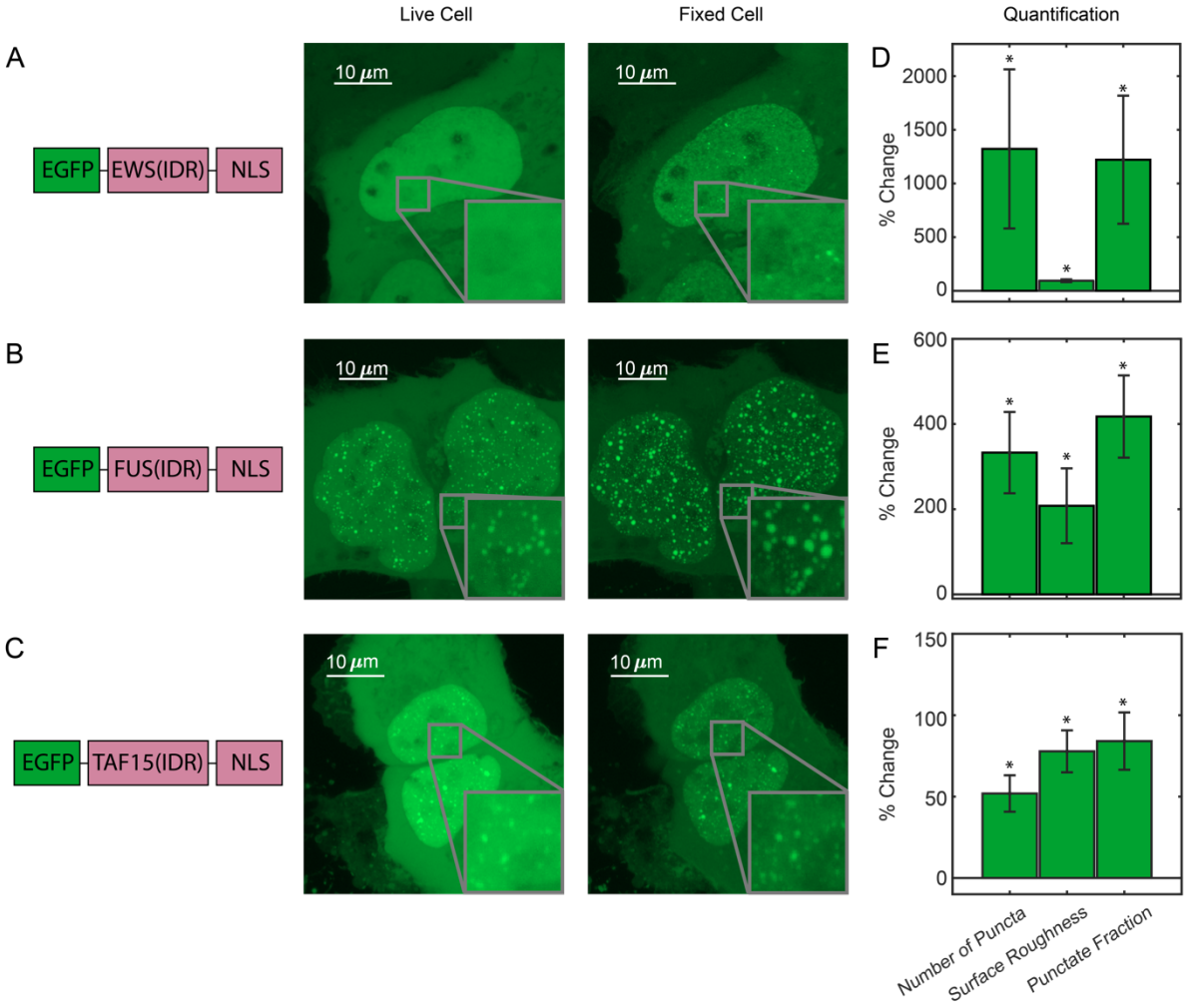

Figure 1. Fixation can change the apparent LLPS behaviors of proteins. (A) EGFP-EWS(IDR), (B) EGFP-FUS(IDR), (C) EGFP-TAF15(IDR) are transiently expressed in U2OS cells and imaged before and after fixation using confocal fluorescence microscopy. A schematic of each protein construct is shown on the left. Maximum z-projections of representative live cells expressing EGFP-FET family protein constructs are shown next to the same cells after 10 minutes of fixation with 4% PFA. The inserts show a zoomed in region of the cell. (D-F) Quantification of percentage change of LLPS parameters after fixation. The values are averaged from 15 (D), 17 (E), or 24 (F) cells. Error bars represent standard errors. Asterisks indicate a significant difference compared with 0 ($P < 0.05$, Wilcoxon signed rank test).

Video 1. **Fixation of U2OS cell over-expressing EGFP-FUS(IDR)**
Download Video1.mp4

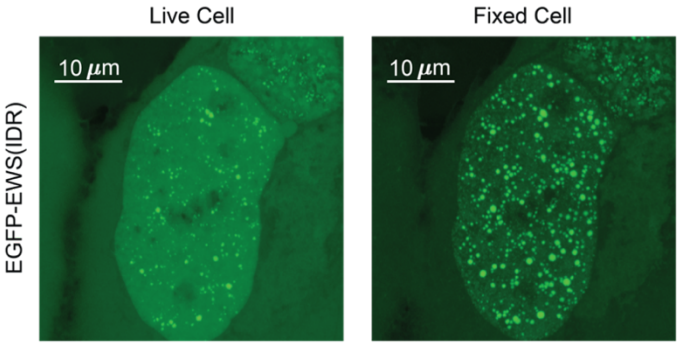

Figure 1–figure supplement 1. EGFP-EWS(IDR) can form droplet-like puncta in living cells. The expression level of EGFP-EWS(IDR) here is significantly higher than in **Figure 1A**. After PFA fixation, additional puncta appear, and pre-existing puncta get bigger and brighter relative to the nucleoplasm, consistent with the trend shown in **Figure 1A**.

We next compared the intracellular distribution of TAF15(IDR) tagged with different fluorescent tags, e.g., EGFP, DsRed2, and HaloTag, before and after fixation. The LLPS behavior of DsRed2-TAF15(IDR) is enhanced upon fixation like EGFP-TAF15(IDR) (**Figure 2A**), but the enhancement has a different appearance. Whereas there is not a significant change to the large pre-formed DsRed2-TAF15(IDR) puncta, thousands of smaller puncta emerge in the dilute phase within the nucleus (**Figure 2B**). In contrast, Halo-TAF15(IDR) displays a diminished LLPS behavior after fixation, with its puncta becoming smaller and dimmer or completely disappearing (**Figure 2C and Figure 2–figure supplement 1**). Quantification of the number of puncta, surface roughness, and punctate fraction of the TAF15(IDR) LLPS systems before and after fixation further confirmed these observations (**Figure 2D-F**). The fact that different phase-separating proteins can have bifurcating behaviors upon fixation is interesting. While it is known that EGFP and DsRed2 can dimerize and HaloTag cannot (Matz et al., 1999; Sacchetti et al., 2002; Zacharias et al., 2002), it is unclear if and how the dimerization potential might contribute to the proteins' bifurcating responses to PFA fixation. We note that the fixation-induced changes to LLPS appearance can affect the physical characterization of *in vivo* LLPS systems based on fixed cell imaging, such as the Gibbs energy of transfer between dilute and concentrated phases (Riback et al., 2020) and how far from the critical concentration a system is (Bracha et al., 2018), potentially affecting the interpretation of the functional role of LLPS in cellular processes. Moreover, the fact that PFA fixation can artificially promote puncta formation even in cells without detectable puncta in the live condition

presents an important caveat in fixation-based approaches that have been commonly used for characterizing LLPS under physiological conditions, e.g., immunofluorescence (Yu et al., 2021).

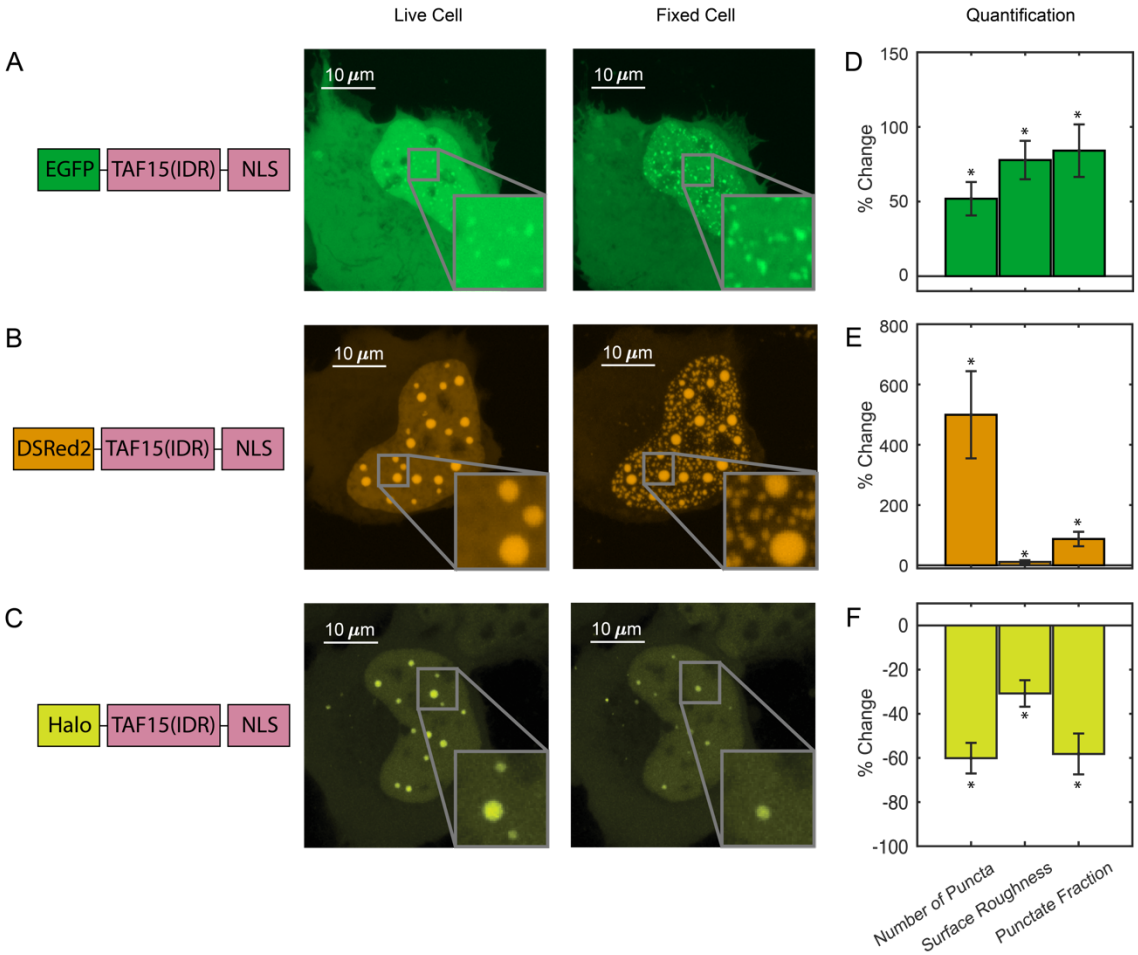

Figure 2. PFA fixation can both enhance and diminish LLPS appearance. U2OS cells expressing (A) EGFP-TAF15(IDR), (B) DsRed2-TAF15(IDR), and (C) Halo-TAF15(IDR), ligated with the JFX549 Halo ligand, are imaged using confocal fluorescence microscopy before and after 10 minutes of fixation with 4% PFA. Schematics of the protein constructs are shown on the left. Live cell images and fixed cell images are compared. (D-F) Quantification of LLPS parameters after fixation. The values are averaged from 24 (D), 23 (E) or 10 (F) cells. Error bars represent standard errors. Asterisks indicate a significant difference compared with 0 ($P < 0.05$, Wilcoxon signed rank test).

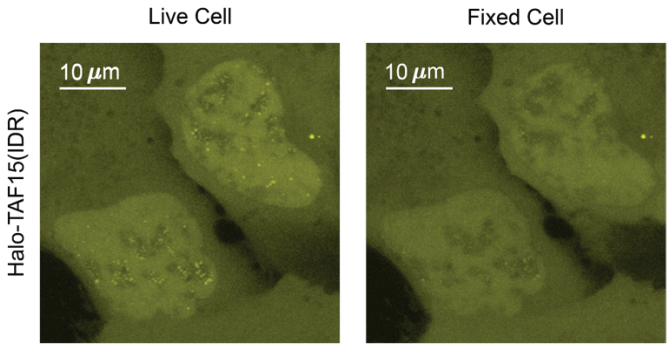

Figure 2–figure supplement 1. Fixation can diminish LLPS appearance. Two U2OS cells expressing Halo-TAF15(IDR) are side-by-side in the same field of view. Puncta formed in live cell nuclei disappeared after fixation.

Furthermore, to examine whether all phase-separating proteins show the fixation artifact, we compared live and fixed cell images of EGFP-tagged full-length FUS (FUS(FL)) expressed in U2OS cells. Full-length FUS is reported to have a greater LLPS propensity *in vitro* than its IDR alone (Wang et al., 2018). We found that EGFP-FUS(FL) overexpressed in live U2OS cells forms many small puncta throughout the nucleus, and we did not observe a significant change of this behavior after PFA fixation (**Figure 3**). This result suggests that PFA fixation does not change the intracellular distribution of all proteins that can phase separate.

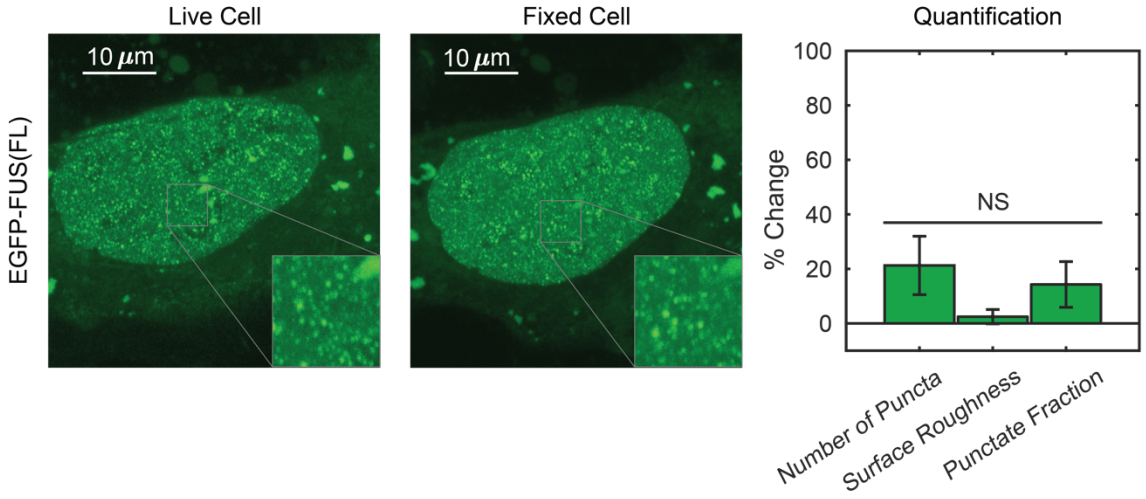

Figure 3. Not all phase-separating proteins show the fixation artifact. EGFP-FUS(FL) does not show significant changes in its LLPS behavior in the fixed cell image as compared to the live cell image. The values are averaged from 21 cells. Error bars represent standard errors. NS: not significant difference compared with 0 ($P < 0.05$, Wilcoxon signed rank test).

Switching between Enhancing and Diminishing Fixation Artifact Depends on Fixation Kinetics

To understand what factors are underlying the diverging fixation artifact of *in vivo* LLPS systems, we perform the above-described fixation imaging assay with glycine added to live cells prior to PFA

fixation. Glycine is highly reactive with formaldehyde and is commonly used to quench the formation of protein-protein cross-linked complexes by quickly forming protein-glycine and glycine-glycine cross-linked adducts instead (Hoffman et al., 2015). We thus utilized additional glycine to generate a competitive fixation reaction in the cell against protein-protein fixation. We found that addition of glycine dramatically reversed the fixation effect on the LLPS behavior of DsRed2-TAF15(IDR) (**Figure 4**). When fixed in the presence of 25 mM glycine, many of the smaller puncta formed in live cells disappear completely and larger, pre-formed puncta turn into a "donut" shape, with the outline of the droplet still visible but the interior devoid of the protein. Neither of these fixed-cell images are good representations of live cells, but it appears that glycine affects the critical parameters that control the divergent artifact of PFA fixation. The observation that the appearance of droplet-like puncta in fixed cells can be dramatically modified by the presence of glycine competition emphasizes that the kinetics of fixation can play an essential role in the appearance of LLPS in fixed cells.

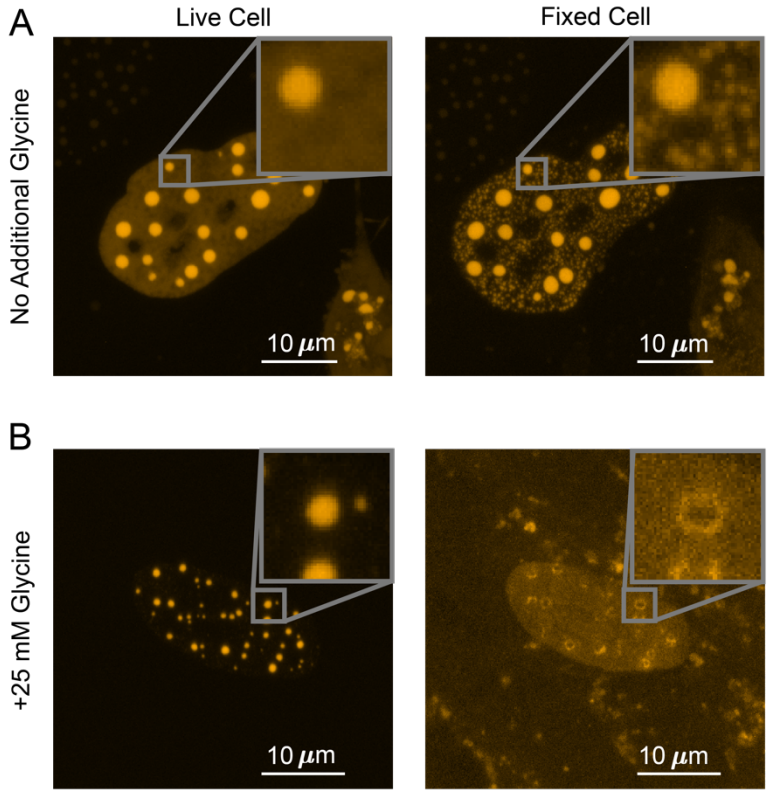

Figure 4. Competitive fixation pathway creates a reversed fixation artifact. (A) Fixing U2OS cells that express DsRed2-TAF15(IDR) in the absence of additional glycine causes many small puncta to appear. (B) Fixing cells in the presence of 25 mM additional glycine results in a reduction in the number of puncta, with large puncta forming "donut" shapes.

Kinetic Modeling Explains the Fixation Artifact

Given our observation that fixation kinetics are critical to the appearance of LLPS in fixed cells, we numerically simulated a 4-state kinetic model (Hoops et al., 2006). As shown in **Figure 5A-B**, the model focuses on one protein of interest (POI), which before fixation can either be in $state_1$ - "in puncta" or $state_2$ - "out of puncta". Because POI molecules are dynamically exchanged in and out of

puncta, the in-puncta fraction of POI is at an equilibrium determined by the ratio of the binding rate, k_1, and the dissociation rate, k_2 (Pollard, 2010). We define the moment that PFA is added as time zero ($t = 0$) and introduce two fixed states of POI, which are $state_3$ (POI cross-linked to proteins within puncta) with a fixation rate of k_3 and $state_4$ (POI cross-linked to proteins outside puncta) with a fixation rate of k_4. Since k_3 and k_4 are both irreversible, the cell will be fully fixed long after PFA fixation ($t = \infty$), when there will no longer be any concentration in $state_1$ and $state_2$. The fixation artifact of an LLPS system can be represented as the absolute change in punctate fraction, or the ratio of in-puncta POI to total POI, after fixation:

$$\Delta Punctate\ Fraction = Final\ Punctate\ Fracion - Starting\ Punctate\ Fraction$$

$$= \left(\frac{[state_3](t=\infty)}{[state_3](t=\infty) + [state_4](t=\infty)} - \frac{[state_1](t=0)}{[state_1](t=0) + [state_2](t=0)} \right) * 100$$

We hypothesized that the balance between interaction and fixation dynamics in a LLPS system causes the fixation artifact and tested the hypothesis by calculating $\Delta\ Punctate\ Fraction$ as a function of various kinetic and equilibrium parameters.

It is well-established that the dilute and concentrated phases of a LLPS system have different protein composition and concentrations (Currie and Rosen, 2022; Koga et al., 2011; Magdalena Estirado et al., 2020; Nott et al., 2015; Yewdall et al., 2021). The rate of fixation is known to vary with both factors by orders of magnitude, with the timescale of fixation ranging from seconds to hours (Hoffman et al., 2015; Kamps et al., 2019; Metz et al., 2006; Metz et al., 2004). Because protein-protein interactions that drive LLPS are highly dynamic with binding residence times in the range of seconds to tens of seconds (Chong et al., 2018), fixation likely happens with either lower or comparable rates than protein binding and dissociation. We thus first examined if different fixation rates of POI in and out of puncta can cause a fixation artifact, assuming the overall fixation rates are slower than protein binding and dissociation, and how the fixation artifact may depend on intrinsic protein-protein interaction equilibrium. Specifically, we calculated $\Delta Punctate\ Fraction$ as a function of the starting punctate fraction and the relative in-puncta fixation rate (k_3: k_4) when the relative overall fixation rate is constant ($(k_3 + k_4)$: $(k_1 + k_2)$=1:5) (**Figure 5C**). In the scenario where the rate of fixation is the same in and out of the puncta ($k_3 = k_4$), the live-cell equilibrium is perfectly preserved in fixed cells regardless of the starting punctate fraction ($\Delta Punctate\ Fraction \sim 0$). However, when one fixation rate is faster than the other, we observe a bifurcating effect. When the fixation rate inside the puncta is greater than outside the puncta ($k_3 > k_4$), the fixed cell will have a higher punctate fraction than the live cell, i.e., fixation enhances the apparent LLPS behaviors. When the balance is reversed ($k_4 > k_3$), the fixed cells will have diminished apparent LLPS behaviors than in the live cell. For cases where the starting punctate fraction is near 0% or 100% due to significantly different POI binding and the dissociation rates ($k_2 \gg k_1$ or $k_1 \gg k_2$), no significant change to LLPS appearance happens after fixation ($\Delta Punctate\ Fraction \sim 0$). In short, our simulation suggests that having unequal fixation rates in and out of puncta is necessary to cause a fixation artifact of LLPS systems and the artifact is dependent on the in-puncta fraction of POI in living cells.

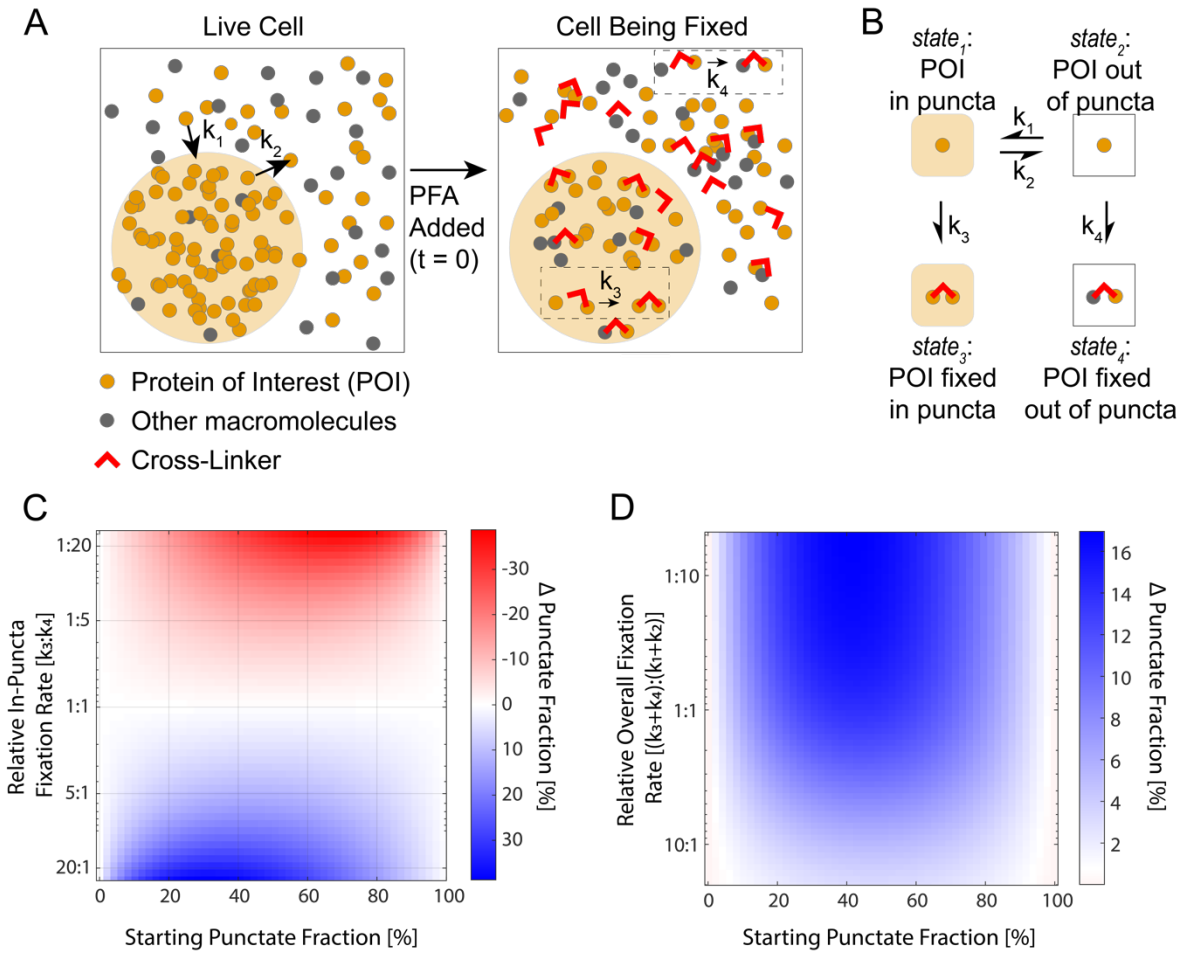

Figure 5. **Kinetic simulation explains bifurcating fixation artifacts**. (A) Schematic that describes fixation of a phase-separating POI in the cell. (B) The four-state kinetic model with associated kinetic rates connecting the different states. (C) Simulation of the fixation artifact as a function of the starting punctate fraction and the relative in-puncta fixation rate k_3: k_4. Faster in-puncta fixation causes LLPS behavior to be over-represented (blue). Slower in-puncta fixation causes LLPS behavior to be under-represented (red). (D) Simulation of the fixation artifact as a function of the starting punctate fraction and the relative overall fixation rate $(k_3 + k_4)$: $(k_1 + k_2)$, assuming k_3: $k_4 = 2$: 1. Fast overall fixation rate compared with protein-protein interaction dynamics decreases the fixation artifact.

Because previous reports have documented that fixation preserves transient interactions worse than stable interactions (Poorey et al., 2013; Schmiedeberg et al., 2009; Teves et al., 2016), we next investigated how fixation rates relative to protein-protein interaction dynamics may impact the observed fixation artifact. Specifically, we calculated $\Delta Punctate\ Fraction$ as a function of both the starting punctate fraction and the relative overall fixation rate, $(k_3 + k_4)$: $(k_1 + k_2)$, assuming a constant relative in-puncta fixation rate (k_3: k_4 =2:1) (**Figure 5D**). Here, a fast relative overall fixation rate can either be caused by slow protein-protein interaction dynamics (low $(k_1 + k_2)$) or fast absolute fixation rates (high $(k_3 + k_4)$). We found when the protein-protein interactions are highly dynamic compared with the overall fixation rates ($(k_3 + k_4) \ll (k_1 + k_2)$), the fixation artifact is the most

pronounced as shown by a large value of $\Delta Punctate\ Fraction$. In contrast, when the protein-protein interactions are stable and less dynamic compared with the overall fixation rate ($(k_3 + k_4) \gg (k_1 + k_2)$), there is a minimal fixation artifact and the punctate fraction in fixed cells is similar to that in living cells ($\Delta Punctate\ Fraction \sim 0$). In short, our simulation suggests that when the overall fixation rate is fast compared with the dynamics of targeted interactions, fixation artifacts can be minimized even with unequal fixation rates in and out of puncta. Our simulated result that less dynamic interactions are better captured by PFA fixation agrees with previously reported experimental observations (Poorey et al., 2013; Schmiedeberg et al., 2009; Teves et al., 2016).

Overall, our kinetic model suggests that the observed fixation artifact of LLPS systems is driven by the interplay of three factors: protein-protein interaction dynamics, the absolute overall fixation rate, and different fixation rates in and out of puncta. Different fixation rates of POI in and out of puncta ($k_3 : k_4 \neq 1:1$) are required for fixation artifacts to happen and the value of $k_3 : k_4$ determines whether the LLPS behavior of POI gets over-represented or under-represented in fixed cell images. The intrinsic rates by which POI binds to and dissociates from its puncta impact the magnitude of fixation artifacts by determining both the live-cell equilibrium of LLPS (starting punctate fraction) and the relative overall fixation rate of POI ($(k_3 + k_4) : (k_1 + k_2)$).

Discussion

Understanding situations in which PFA fixation can properly preserve live-cell conditions is essential in judicious applications of fixation-based biological techniques. Because approaches for rigorous determination of LLPS *in vivo* remain lacking (McSwiggen et al., 2019) and detection of local high-concentration regions of an endogenously expressed protein in fixed cells via immunofluorescence has been widely used as evidence for LLPS (Hayes and Weeks, 2016; Kato et al., 2012; Lin et al., 2016; Maharana et al., 2018; Sabari et al., 2018; Wang et al., 2021; Yang et al., 2020), understanding how well fixation preserves LLPS behaviors is important for justifying the immunofluorescence-based diagnosis method and for studying the functional relevance of LLPS *in vivo*. In this work, we imaged various LLPS systems in living cells before and after PFA fixation, quantified parameters that describe LLPS appearance in cells, and showed that fixation can either enhance or diminish the apparent LLPS behaviors *in vivo*. For the first time, our work reveals an important caveat in using fixation-based methods to detect and characterize LLPS *in vivo* and suggests an advantage of using live-cell imaging to study LLPS systems over fixed-cell experiments. However, not all phase-separating proteins have their apparent LLPS behaviors in cells changed upon fixation. For example, PFA fixation faithfully preserves the appearance of EGFP-FUS(FL) puncta in cells (**Figure 3**). Nevertheless, our work points out a necessity to use live-cell imaging to confirm LLPS behaviors previously characterized with fixed-cell experiments.

We note that fixation-induced changes of LLPS appearance may lead to potential misinterpretation of the functional relevance of LLPS in cellular processes. For example, recent work has uncovered that effective transcriptional activation requires an optimum of TF IDR-IDR interactions within TF hubs formed at target genes and that overly high levels of IDR-IDR interactions pushing the system toward LLPS can repress transcription (Chong et al., 2022). Future characterization of the functionally optimal interaction level will require quantification of the sizes of hubs or droplet-like puncta while measuring transcription activity. Because a fixation-induced increase or decrease in puncta sizes may lead to inaccurate determination of the functional optimum, scrutiny will be required in choosing between live-cell and fixed-cell imaging methods for quantifying LLPS appearance in these

types of studies. Moreover, given that fixation can artificially generate intranuclear puncta of EGFP-EWS(IDR) that is homogenously distributed across the live cell nucleus (**Figure 1A**), extra caution is required in interpreting immunofluorescence-detected intracellular puncta of an endogenously expressed protein as LLPS, as the same puncta-generating fixation artifact might happen to the protein even when it is not phase separating in living cells. To confirm puncta formation, counterpart live-cell imaging of the endogenous protein will be necessary, which requires engineering the cells, e.g., by CRISPR, to fluorescently tag the protein.

To understand the factors that can cause fixation-induced changes of LLPS appearance in the cell, we simulated the changes through kinetic modeling, which reveals that the dynamics of POI binding to and dissociating from puncta, the absolute fixation rate of POI, and different fixation rates of POI in and out of puncta all play a role in inducing the fixation artifacts. Our kinetic model takes previous work studying fixation artifacts in the context of protein-DNA interactions (Poorey et al., 2013; Schmiedeberg et al., 2009; Teves et al., 2016) one step further by considering two fixed states of POI instead of one state, which are fixation in and out of puncta with different rates due to distinct local protein composition and concentrations. Because our four-state model makes no assumptions about any state being phase-separated, the logical implications of our model can extend beyond LLPS to other biomolecular transactions, e.g., other protein-protein and protein-nucleic acid interactions. Generally, fixation artifacts will occur whenever a protein can exist in multiple states that have different rates of fixation, and this artifact is most severe when the fixation is slower than the transition between states. Because the PFA fixation rate is sensitively dependent on the amino acid sequence of POI, the structure of POI, and POI's cross-linked partners (Hoffman et al., 2015; Kamps et al., 2019; Metz et al., 2006; Metz et al., 2004), POI in different states should generally have different fixation rates regardless of the type of interaction.

One distinction between our study and previous studies is that we observe that fixation can enhance apparent protein-protein interactions or LLPS behaviors in the cell, suggesting faster fixation for POI in the bound than dissociated state ($k_3 > k_4$), whereas fixation has only been reported to diminish protein-DNA interactions, suggesting slower fixation for POI in the bound state ($k_3 < k_4$) (Poorey et al., 2013; Schmiedeberg et al., 2009; Teves et al., 2016). We hypothesize that this is because fixing the bound state of an LLPS system (within puncta) is dominated by cross-linking reactions between IDRs enriched in puncta, which have reactive residues better exposed to solvent due to lack of well-defined tertiary structures and thereby likely cross-link faster than structured domains cross-linking to DNA (Hoffman et al., 2015). It will be of future interest to measure fixation rates of different biomolecules including IDRs, structured proteins, and nucleic acids to prove the proposed chemical mechanism underlying fixation artifacts. Since our simulated results highlight the role of absolute fixation rates in the outcome of fixation, another future endeavor will be to design novel fixatives with significantly faster cross-linking rates than biomolecular interactions to eliminate fixation artifacts in the cell.

Materials and Methods

Cell Line and Sample Preparation. U2OS cells were grown in 1 g/L DMEM media (ThermoFisher, 10567014) supplemented with 10% FBS (Fisher Scientific, SH3039603) and 1% penicillin-streptomycin (ThermoFisher, 15140122). The cells were split onto an imaging plate (Mattek, P35G-1.5-14-C) and

transfected with fluorescent protein constructs with Lipofectamine 3000 (Fisher Scientific, L3000001) according to manufacturer's instructions. One day after transfection, the culture media was changed to phenol red free DMEM (ThermoFisher, 11054001) with 10% FBS and 1% penicillin-streptomycin. For experiments with additional glycine, glycine (Fisher Scientific, BP381-5) was added to the phenol red free media so that the final concentration was 50 mM (and 25 mM after the addition of 8% PFA, see below). It should be noted that normal DMEM media already contains 0.4 mM glycine.

Fluorescence Microscopy. Confocal fluorescence microscopy was performed on Zeiss LSM 980 in the point-scanning mode with a 63x oil objective (Zeiss, 421782-9900-000). The pinhole was set to 1 airy unit for different emission wavelengths. The images displayed in the manuscript are maximum z-projections of z-stack images. The culture dish contained 1 mL of phenol red free media, so that when 1 mL of 8% paraformaldehyde (PFA) (VWR, 100503-917), the final concentration of PFA was 4%. After waiting 10 mins to allow PFA fixation to complete, images of the same cells are taken again. For experiments with glycine, the final concentration of glycine after PFA addition was 25 mM and 8% PFA was used so that PFA was still in molar excess.

LLPS Parameter Quantification. The three parameters we quantified were the number of puncta, surface roughness, and punctate fraction. To best compare the images of a cell before and after fixation, the two z-projection images were normalized so that the sum of the intensities within the nucleus is equal to 1. The border of the nucleus was manually drawn for each image. All analysis is done on normalized maximum z-projection images except for when calculating punctate fraction. We measured the number of puncta by quantifying the number of peaks within the nucleus. Specifically, the image was exported from MATLAB into ImageJ (Schindelin et al., 2012) using MIJ (Sage et al., 2012), and the "find maxima" processing function was used (**Methods–figure supplement 1**) with the same noise tolerance for both the live and fixed cell images.

To quantify the surface roughness of a cell nucleus image, the standard deviation of fluorescence intensities in the nucleus were compared before and after fixation (**Methods–figure supplement 2**). Utilizing this method of comparing images before and after fixation allows for quantification of change of nucleoplasm without peak fitting. The addition of structures such as LLPS droplets within a chosen patch will increase the standard deviation. Nuclei with puncta resulted in skewed (non-normal) distributions of intensities (Jachowicz et al., 2021), leading to higher standard deviations.

The punctate fraction was determined with the first few steps identical to measuring the number of puncta as described above. The border of the nucleus was manually identified, the images were normalized, and preliminary peak locations were identified on maximum z-projection images using the "find maxima" function in ImageJ. The "find maxima" function does not pick the perfect center of each punctum. Thus, to measure the full width at half maximum (FWHM) of a punctum, we made 36 different radial slices of the punctum crossing the preliminary punctum center pixel, extracted the intensity profile for each radial slice to calculate the punctum's FWHM, and selected the highest FWHM as the corresponding radial slice must have gone through the true center of the punctum. We then made a sum z-projection of the z-stack images, drew a circle with the maximum FWHM as its diameter centering the true central pixel of each punctum on the sum image, and integrated the fluorescence intensity across all circles. (**Methods–figure supplement 3**). The punctate fraction is calculated by dividing the in-circle total fluorescence intensity with the total fluorescence intensity integrated across the nucleus in the sum image.

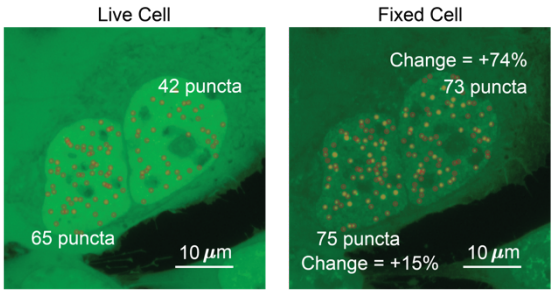

Methods–figure supplement 1. Determination of the number of puncta in the cell nucleus. Two cells expressing EGFP-TAF15(IDR) have the number of puncta before and after fixation compared. The cell on the left shows an increase of 10 puncta, a change of 15%. The cell on the right shows a change of 31 puncta, a change of 74%.

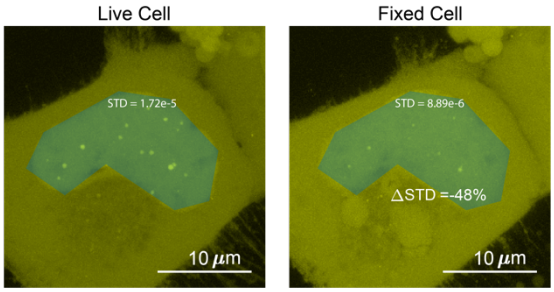

Methods–figure supplement 2. Determination of the surface roughness of a cell nucleus image. We drew a blue patch that covers the nucleus of a cell expressing Halo-TAF15(IDR) and compared the standard deviation of the pixel intensity within the blue patch before and after fixation. The change in standard deviation between the two images is -48%.

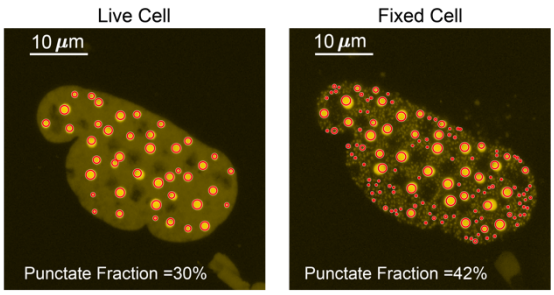

Methods–figure supplement 3. Determination of the punctate fraction. The punctate fraction of DsRed2-TAF15(IDR) is compared before and after fixation. The red circles represent the boundary within which the integrated fluorescence is considered “in puncta”.

Statistical Analysis. Statistical significance was calculated using the Wilcoxon signed rank test (Gibbons and Chakraborti, 2014), a non-parametric version of the one sample Student’s t-test. The reason for using a non-parametric test was because the data often did not have a normal distribution. Cells that did not have many puncta before, like the one shown in **Figure 1A**, resulted in extreme outliers that resulted in skewed distributions. The Wilcoxon signed rank test was performed using the built-in MATLAB function *signrank*.

Kinetic Simulation. A four-state kinetic model was constructed in COPASI (Hoops et al., 2006) and interfaced using Python. The four states and kinetic rates are defined in the main text and **Figure 5B**. We assume a constant total molarity for all species, i.e., $[state_1] + [state_2] + [state_3] + [state_4] = 1\,mol/L$. At $t = 0$, $[state_3] = [state_4] = 0$, while k_1 and k_2 together define the equilibrium between $state_1$ and $state_2$, i.e., $K_{eq} = k_1/k_2 = [state_1]_{eq}/[state_2]_{eq}$. COPASI numerically simulates the four states in the kinetic model utilizing the starting concentrations and rate conditions.

The units used for all the rates were s^{-1}, set so that fixation occurred on the order of seconds. For the simulations that produced **Figure 5C**, we varied the values of k_3 and k_4 but kept the total fixation and POI binding and dissociation rates constant ($k_3 + k_4$ = 0.2, $k_1 + k_2 = 1$), leading to a constant relative overall fixation rate of POI ($(k_3 + k_4)$: $(k_1 + k_2)$=1:5). For the simulations that produced **Figure 5D**, we kept the fixation rates constant ($k_3 = 2$, $k_4 = 1$) and varied the relative overall fixation rate of POI ($(k_3 + k_4)$: $(k_1 + k_2)$). In this simulation, the relative overall fixation rate of POI ($(k_3 + k_4)$: $(k_1 + k_2)$) is set so that the range of interaction rates span values that are an order of magnitude faster and slower than fixation rates.

Acknowledgements

This work was supported by the Shurl and Kay Curci Foundation (to S. Chong) and the John D. Baldeschwieler and Marlene R. Konnar Foundation (to S. Chong). We thank the Caltech Biological Imaging Facility and G. Spigolon for providing technical assistance on confocal fluorescence microscopy. We thank Robert Tjian, Thomas Graham, John Ferrie, Jonathan Karr, and Shawn Yoshida for critical comments on the manuscript.

Conflict of Interests

No competing interests declared.

Materials Availability Statement

The materials described in this study are available on request.

References

Alberti, S., Gladfelter, A., and Mittag, T. (2019). Considerations and challenges in studying liquid-liquid phase separation and biomolecular condensates. Cell *176*, 419-434.
Altmeyer, M., Neelsen, K.J., Teloni, F., Pozdnyakova, I., Pellegrino, S., Grøfte, M., Rask, M.-B.D., Streicher, W., Jungmichel, S., and Nielsen, M.L. (2015). Liquid demixing of intrinsically disordered proteins is seeded by poly (ADP-ribose). Nature communications *6*, 1-12.
Banani, S.F., Lee, H.O., Hyman, A.A., and Rosen, M.K. (2017). Biomolecular condensates: organizers of cellular biochemistry. Nature reviews Molecular cell biology *18*, 285-298.
Berry, J., Weber, S.C., Vaidya, N., Haataja, M., and Brangwynne, C.P. (2015). RNA transcription modulates phase transition-driven nuclear body assembly. Proceedings of the National Academy of Sciences *112*, E5237-E5245.
Boeynaems, S., Alberti, S., Fawzi, N.L., Mittag, T., Polymenidou, M., Rousseau, F., Schymkowitz, J., Shorter, J., Wolozin, B., and Van Den Bosch, L. (2018). Protein phase separation: a new phase in cell biology. Trends in cell biology *28*, 420-435.

Bracha, D., Walls, M.T., Wei, M.-T., Zhu, L., Kurian, M., Avalos, J.L., Toettcher, J.E., and Brangwynne, C.P. (2018). Mapping local and global liquid phase behavior in living cells using photo-oligomerizable seeds. Cell *175*, 1467-1480. e1413.
Chen, F., Tillberg, P.W., and Boyden, E.S. (2015). Expansion microscopy. Science *347*, 543-548.
Choi, J.-M., Holehouse, A.S., and Pappu, R.V. (2020). Physical principles underlying the complex biology of intracellular phase transitions. Annual Review of Biophysics *49*, 107-133.
Chong, S., Dugast-Darzacq, C., Liu, Z., Dong, P., Dailey, G.M., Cattoglio, C., Heckert, A., Banala, S., Lavis, L., and Darzacq, X. (2018). Imaging dynamic and selective low-complexity domain interactions that control gene transcription. Science *361*, eaar2555.
Chong, S., Graham, T.G.W., Dugast-Darzacq, C., Dailey, G.M., Darzacq, X., and Tjian, R. (2022). Tuning levels of low-complexity domain interactions to modulate endogenous oncogenic transcription. Molecular Cell *82*, 1-14.
Currie, S.L., and Rosen, M.K. (2022). Using quantitative reconstitution to investigate multicomponent condensates. RNA *28*, 27-35.
Gavrilov, A., Razin, S.V., and Cavalli, G. (2015). In vivo formaldehyde cross-linking: it is time for black box analysis. Briefings in functional genomics *14*, 163-165.
Gibbons, J.D., and Chakraborti, S. (2014). Nonparametric statistical inference (CRC press).
Gibbs, J.W. (1879). On the equilibrium of heterogeneous substances.
Graham, T. (1861). X. Liquid diffusion applied to analysis. Philosophical transactions of the Royal Society of London, 183-224.
Hayes, M.H., and Weeks, D.L. (2016). Amyloids assemble as part of recognizable structures during oogenesis in Xenopus. Biology open *5*, 801-806.
Hoffman, E.A., Frey, B.L., Smith, L.M., and Auble, D.T. (2015). Formaldehyde crosslinking: a tool for the study of chromatin complexes. Journal of Biological Chemistry *290*, 26404-26411.
Hoops, S., Sahle, S., Gauges, R., Lee, C., Pahle, J., Simus, N., Singhal, M., Xu, L., Mendes, P., and Kummer, U. (2006). COPASI—a complex pathway simulator. Bioinformatics *22*, 3067-3074.
Hyman, A.A., Weber, C.A., and Jülicher, F. (2014). Liquid-liquid phase separation in biology. Annual review of cell and developmental biology *30*, 39-58.
Jachowicz, J.W., Strehle, M., Banerjee, A.K., Thai, J., Blanco, M.R., and Guttman, M. (2021). Xist spatially amplifies SHARP recruitment to balance chromosome-wide silencing and specificity to the X chromosome.
Kamps, J.J., Hopkinson, R.J., Schofield, C.J., and Claridge, T.D. (2019). How formaldehyde reacts with amino acids. Communications Chemistry *2*, 1-14.
Kato, M., Han, T.W., Xie, S., Shi, K., Du, X., Wu, L.C., Mirzaei, H., Goldsmith, E.J., Longgood, J., and Pei, J. (2012). Cell-free formation of RNA granules: low complexity sequence domains form dynamic fibers within hydrogels. Cell *149*, 753-767.
Kato, M., and McKnight, S.L. (2018). A solid-state conceptualization of information transfer from gene to message to protein. Annual review of biochemistry *87*, 351-390.
Koga, S., Williams, D.S., Perriman, A.W., and Mann, S. (2011). Peptide–nucleotide microdroplets as a step towards a membrane-free protocell model. Nature chemistry *3*, 720-724.
Kwon, I., Kato, M., Xiang, S., Wu, L., Theodoropoulos, P., Mirzaei, H., Han, T., Xie, S., Corden, J.L., and McKnight, S.L. (2013). Phosphorylation-regulated binding of RNA polymerase II to fibrous polymers of low-complexity domains. Cell *155*, 1049-1060.
Li, P., Banjade, S., Cheng, H.-C., Kim, S., Chen, B., Guo, L., Llaguno, M., Hollingsworth, J.V., King, D.S., and Banani, S.F. (2012). Phase transitions in the assembly of multivalent signalling proteins. Nature *483*, 336-340.
Lin, Y., Mori, E., Kato, M., Xiang, S., Wu, L., Kwon, I., and McKnight, S.L. (2016). Toxic PR poly-dipeptides encoded by the C9orf72 repeat expansion target LC domain polymers. Cell *167*, 789-802. e712.

Magdalena Estirado, E., Mason, A.F., Alemán García, M.A.n., van Hest, J.C., and Brunsveld, L. (2020). Supramolecular nanoscaffolds within cytomimetic protocells as signal localization hubs. Journal of the American Chemical Society *142*, 9106-9111.
Maharana, S., Wang, J., Papadopoulos, D.K., Richter, D., Pozniakovsky, A., Poser, I., Bickle, M., Rizk, S., Guillén-Boixet, J., and Franzmann, T.M. (2018). RNA buffers the phase separation behavior of prion-like RNA binding proteins. Science *360*, 918-921.
Matz, M.V., Fradkov, A.F., Labas, Y.A., Savitsky, A.P., Zaraisky, A.G., Markelov, M.L., and Lukyanov, S.A. (1999). Fluorescent proteins from nonbioluminescent Anthozoa species. Nature biotechnology *17*, 969-973.
McSwiggen, D.T., Mir, M., Darzacq, X., and Tjian, R. (2019). Evaluating phase separation in live cells: diagnosis, caveats, and functional consequences. Genes & development *33*, 1619-1634.
Metz, B., Kersten, G.F., Baart, G.J., de Jong, A., Meiring, H., ten Hove, J., van Steenbergen, M.J., Hennink, W.E., Crommelin, D.J., and Jiskoot, W. (2006). Identification of formaldehyde-induced modifications in proteins: reactions with insulin. Bioconjugate chemistry *17*, 815-822.
Metz, B., Kersten, G.F., Hoogerhout, P., Brugghe, H.F., Timmermans, H.A., De Jong, A., Meiring, H., ten Hove, J., Hennink, W.E., and Crommelin, D.J. (2004). Identification of formaldehyde-induced modifications in proteins: reactions with model peptides. Journal of Biological Chemistry *279*, 6235-6243.
Mitrea, D.M., and Kriwacki, R.W. (2016). Phase separation in biology; functional organization of a higher order. Cell Communication and Signaling *14*, 1-20.
Moter, A., and Göbel, U.B. (2000). Fluorescence in situ hybridization (FISH) for direct visualization of microorganisms. Journal of microbiological methods *41*, 85-112.
Nott, T.J., Petsalaki, E., Farber, P., Jervis, D., Fussner, E., Plochowietz, A., Craggs, T.D., Bazett-Jones, D.P., Pawson, T., and Forman-Kay, J.D. (2015). Phase transition of a disordered nuage protein generates environmentally responsive membraneless organelles. Molecular cell *57*, 936-947.
Pollard, T.D. (2010). A guide to simple and informative binding assays. Molecular biology of the cell *21*, 4061-4067.
Poorey, K., Viswanathan, R., Carver, M.N., Karpova, T.S., Cirimotich, S.M., McNally, J.G., Bekiranov, S., and Auble, D.T. (2013). Measuring chromatin interaction dynamics on the second time scale at single-copy genes. Science *342*, 369-372.
Quinodoz, S.A., Ollikainen, N., Tabak, B., Palla, A., Schmidt, J.M., Detmar, E., Lai, M.M., Shishkin, A.A., Bhat, P., and Takei, Y. (2018). Higher-order inter-chromosomal hubs shape 3D genome organization in the nucleus. Cell *174*, 744-757. e724.
Richter, K.N., Revelo, N.H., Seitz, K.J., Helm, M.S., Sarkar, D., Saleeb, R.S., d'Este, E., Eberle, J., Wagner, E., and Vogl, C. (2018). Glyoxal as an alternative fixative to formaldehyde in immunostaining and super‐resolution microscopy. The EMBO journal *37*, 139-159.
Rust, M.J., Bates, M., and Zhuang, X. (2006). Sub-diffraction-limit imaging by stochastic optical reconstruction microscopy (STORM). Nature methods *3*, 793-796.
Sabari, B.R., Dall'Agnese, A., Boija, A., Klein, I.A., Coffey, E.L., Shrinivas, K., Abraham, B.J., Hannett, N.M., Zamudio, A.V., and Manteiga, J.C. (2018). Coactivator condensation at super-enhancers links phase separation and gene control. Science *361*, eaar3958.
Sacchetti, A., Subramaniam, V., Jovin, T.M., and Alberti, S. (2002). Oligomerization of DsRed is required for the generation of a functional red fluorescent chromophore. FEBS letters *525*, 13-19.
Sage, D., Prodanov, D., Tinevez, J.-Y., and Schindelin, J. (2012). MIJ: making interoperability between ImageJ and Matlab possible. In ImageJ User & Developer Conference.
Schindelin, J., Arganda-Carreras, I., Frise, E., Kaynig, V., Longair, M., Pietzsch, T., Preibisch, S., Rueden, C., Saalfeld, S., and Schmid, B. (2012). Fiji: an open-source platform for biological-image analysis. Nature methods *9*, 676-682.

Schmiedeberg, L., Skene, P., Deaton, A., and Bird, A. (2009). A temporal threshold for formaldehyde crosslinking and fixation. PLoS One *4*, e4636.
Schuster, B.S., Dignon, G.L., Tang, W.S., Kelley, F.M., Ranganath, A.K., Jahnke, C.N., Simpkins, A.G., Regy, R.M., Hammer, D.A., and Good, M.C. (2020). Identifying sequence perturbations to an intrinsically disordered protein that determine its phase-separation behavior. Proceedings of the National Academy of Sciences *117*, 11421-11431.
Shin, Y., and Brangwynne, C.P. (2017). Liquid phase condensation in cell physiology and disease. Science *357*, eaaf4382.
Shishodia, S., Zhang, D., El-Sagheer, A., Brown, T., Claridge, T., Schofield, C., and Hopkinson, R. (2018). NMR analyses on N-hydroxymethylated nucleobases–implications for formaldehyde toxicity and nucleic acid demethylases. Organic & biomolecular chemistry *16*, 4021-4032.
Solomon, M.J., and Varshavsky, A. (1985). Formaldehyde-mediated DNA-protein crosslinking: a probe for in vivo chromatin structures. Proceedings of the National Academy of Sciences *82*, 6470-6474.
Stadler, C., Skogs, M., Brismar, H., Uhlén, M., and Lundberg, E. (2010). A single fixation protocol for proteome-wide immunofluorescence localization studies. Journal of Proteomics *73*, 1067-1078.
Sutherland, B.W., Toews, J., and Kast, J. (2008). Utility of formaldehyde cross ‐ linking and mass spectrometry in the study of protein ‐ protein interactions. Journal of mass spectrometry *43*, 699-715.
Teves, S.S., An, L., Hansen, A.S., Xie, L., Darzacq, X., and Tjian, R. (2016). A dynamic mode of mitotic bookmarking by transcription factors. Elife *5*, e22280.
Wang, J., Choi, J.-M., Holehouse, A.S., Lee, H.O., Zhang, X., Jahnel, M., Maharana, S., Lemaitre, R., Pozniakovsky, A., and Drechsel, D. (2018). A molecular grammar governing the driving forces for phase separation of prion-like RNA binding proteins. Cell *174*, 688-699. e616.
Wang, J., Shi, C., Xu, Q., and Yin, H. (2021). SARS-CoV-2 nucleocapsid protein undergoes liquid–liquid phase separation into stress granules through its N-terminal intrinsically disordered region. Cell discovery *7*, 1-5.
Yang, P., Mathieu, C., Kolaitis, R.-M., Zhang, P., Messing, J., Yurtsever, U., Yang, Z., Wu, J., Li, Y., and Pan, Q. (2020). G3BP1 is a tunable switch that triggers phase separation to assemble stress granules. Cell *181*, 325-345. e328.
Yewdall, N.A., André, A.A., Lu, T., and Spruijt, E. (2021). Coacervates as models of membraneless organelles. Current Opinion in Colloid & Interface Science *52*, 101416.
Yu, C., Shen, B., You, K., Huang, Q., Shi, M., Wu, C., Chen, Y., Zhang, C., and Li, T. (2021). Proteome-scale analysis of phase-separated proteins in immunofluorescence images. Briefings in bioinformatics *22*, bbaa187.
Zacharias, D.A., Violin, J.D., Newton, A.C., and Tsien, R.Y. (2002). Partitioning of lipid-modified monomeric GFPs into membrane microdomains of live cells. Science *296*, 913-916.
Zheng, W., Dignon, G.L., Jovic, N., Xu, X., Regy, R.M., Fawzi, N.L., Kim, Y.C., Best, R.B., and Mittal, J. (2020). Molecular details of protein condensates probed by microsecond long atomistic simulations. The Journal of Physical Chemistry B *124*, 11671-11679.